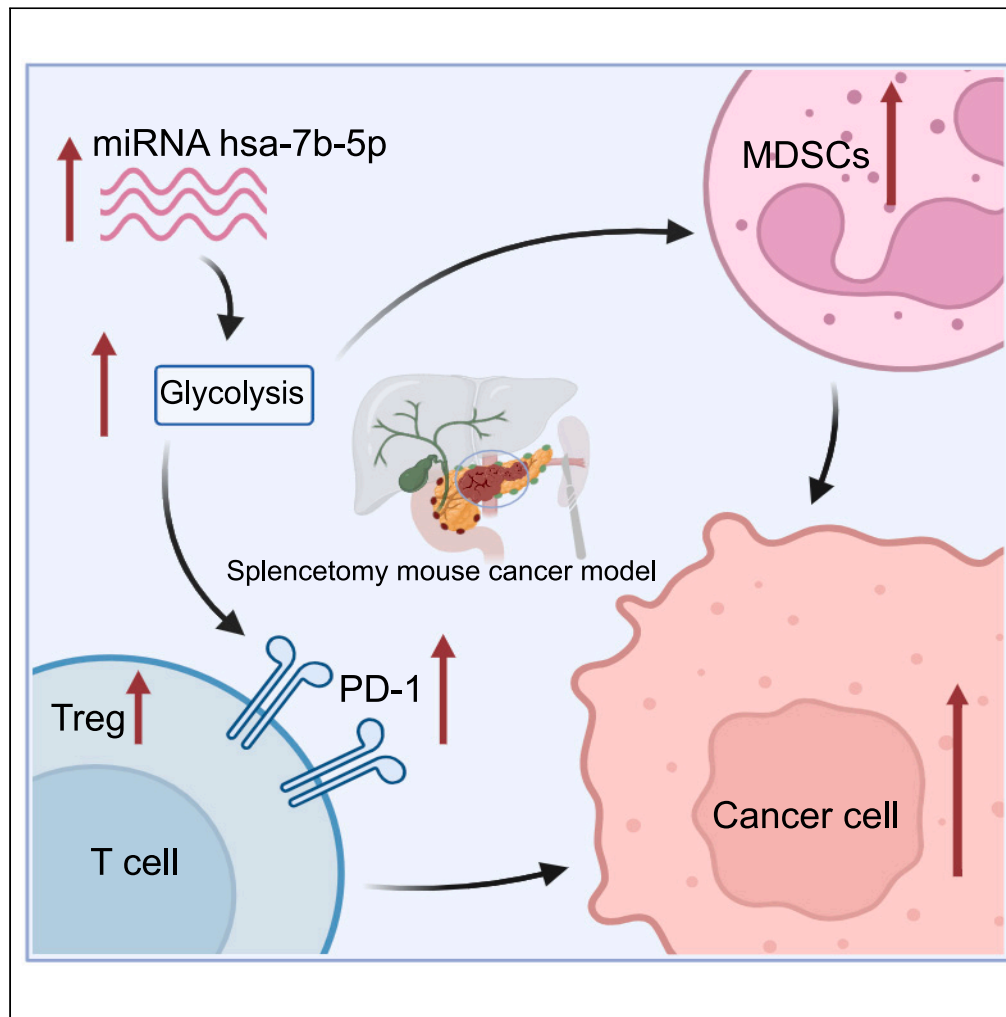**Article**

Revealing splenectomy-driven microRNA hsa-7b-5p's role in pancreatic cancer progression

Liangliang Wu,
Yongjie Xie, Bo Ni,
..., Chengyan Wu,
Yuexiang Liang,
Xiaona Wang

wangxiaona0520@126.com

Highlights

Splenectomy promotes the progression of PDAC

High expression of miRNA hsa-7b-5p in tumor post-splenectomy

Hsa-7b-5p linked to cancer staging and immunosuppressive status

Hsa-7b-5p may serve as a prognostic biomarker and therapeutic target for PDAC

Article

Revealing splenectomy-driven microRNA hsa-7b-5p's role in pancreatic cancer progression

Liangliang Wu,[1,5] Yongjie Xie,[2,5] Bo Ni,[2,5] Peng Jin,[1] Bin Li,[1] Mingzhi Cai,[1] Baogui Wang,[1] Chengyan Wu,[3] Yuexiang Liang,[4] and Xiaona Wang[1,6,*]

SUMMARY

Splenectomy often accompanies distal pancreatectomy for pancreatic cancer. However, debates persist on splenic function loss impact. Prior studies in mice revealed splenectomy promotes pancreatic cancer growth by altering CD4/Foxp3 and CD8/Foxp3 ratios. The effect on other immune cells remains unclear. Clinical observations indicate splenectomy induces immunosuppression, heightening recurrence and metastasis risk. Here, we established an orthotopic pancreatic cancer model with splenectomy and observed a significant increase in tumor burden. Flow cytometry revealed elevated MDSCs, CD8+PD-1high+ T cells, and reduced CD4+ T cells, CD8+ T cells, and natural killer cells in tumors. Bulk sequencing identified increased MicroRNA (miRNA) hsa-7b-5p post-splenectomy, correlating with staging and immunosuppression. Similar results were obtained *in vivo* by constructing a KPC-miRNA hsa-7b-5p-sh cell line. These findings suggest that splenectomy enhances the expression of miRNA hsa-7b-5p, inhibits the tumor immune microenvironment, and promotes pancreatic cancer growth.

INTRODUCTION

Pancreatic cancer is the most lethal human solid tumor, with a 5-year survival rate of less than 10%.[1,2] Splenectomy is often performed during the treatment of PDAC located at the head or tail of the pancreas due to the anatomical relationship and the influence of lymph node metastasis. However, spleen deficiency may lead to a decline in immune function and complications such as anemia and infection in patients with pancreatic cancer.[3,4] MicroRNAs (miRNAs) are non-coding RNA molecules that regulate the transcription and translation of target genes, affecting various biological processes in cells.[5–7] Abnormal miRNA expression is closely related to many diseases, especially cancer.[8–15] Previous studies have found that splenectomy alters miRNA expression profiles and that the regulation of some miRNAs after splenectomy may be related to physiological processes such as inflammation, immunity, erythropoiesis, and metabolic regulation.[16–19] Hsa-7b-5p is a small RNA molecule that is involved in a variety of biological processes, including the regulation of gene expression and cell proliferation and therapeutic target for cancer.[20] It is involved in the regulation of genes required for Severe Acute Respiratory Syndrome Coronavirus-2 (SARS-CoV-2) infection and may be a therapeutic target for coronavirus disease (COVID-19).[21] In various cancers, the high expression level of hsa-7b-5p is closely related to the degree of malignancy and prognosis.[22,23] Nevertheless, the relationship between hsa-7b-5p and splenectomy remains poorly understood. In rats, splenectomy experiments have altered the expression profiles of many miRNAs, including hsa-7b-5p, which may be involved in different physiological regulation processes at different time points after splenectomy. Hsa-7b-5p is considered to be a potential cancer marker and therapeutic target. In breast cancer, colorectal cancer, liver cancer, gastric cancer and other cancers, the expression level of hsa-7b-5p is significantly increased. Moreover, the high expression level is closely related to the malignant degree and prognosis of the tumor. It can also affect the number of tumor cells and immune tolerance by regulating the apoptosis and proliferation of tumor cells. In addition, some studies have shown that Hsa-7b-5p can also regulate the functions of regulatory T cells, natural killer cells and dendritic cells, thereby affecting the immune response of tumors.

Therefore, Hsa-7b-5p is considered to be a potential target for tumor immunotherapy. By regulating the expression level of Hsa-7b-5p, it may help to enhance the tumor immune response and improve the efficacy of tumor therapy. In summary, has-let-7b-5p demonstrates diverse functions in various cancers and diseases. It may act as a diagnostic biomarker and therapeutic target in AML, NSCLC, and glioblastoma, while being associated with inflammation and apoptosis in pulmonary embolism (PE).[24–28] However, there is still no sufficient research to support the specific relationship between Hsa-let-7b-5p and splenectomy, and further research is needed to reveal the specific mechanism of action of Hsa-7b-5p in the immune microenvironment of pancreatic cancer.

[1]Department of Gastric Cancer, Tianjin Medical University Cancer Institute and Hospital, National Clinical Research Center for Cancer, Key Laboratory of Cancer Prevention and Therapy, Tianjin 300060, China
[2]Department of Pancreatic Cancer, Tianjin Medical University Cancer Institute and Hospital, National Clinical Research Center for Cancer; Key Laboratory of Cancer Prevention and Therapy, Tianjin's Clinical Research Center for Cancer, Tianjin 300060, China
[3]Department of Bioinformation, Beijing University of Technology, Beijing 100124, China
[4]Department of Gastrointestinal Oncology, The First Affiliated Hospital of Hainan Medical University, Longhua Road, Longhua District, Haikou 570102, China
[5]These authors contributed equally
[6]Lead contact
*Correspondence: wangxiaona0520@126.com
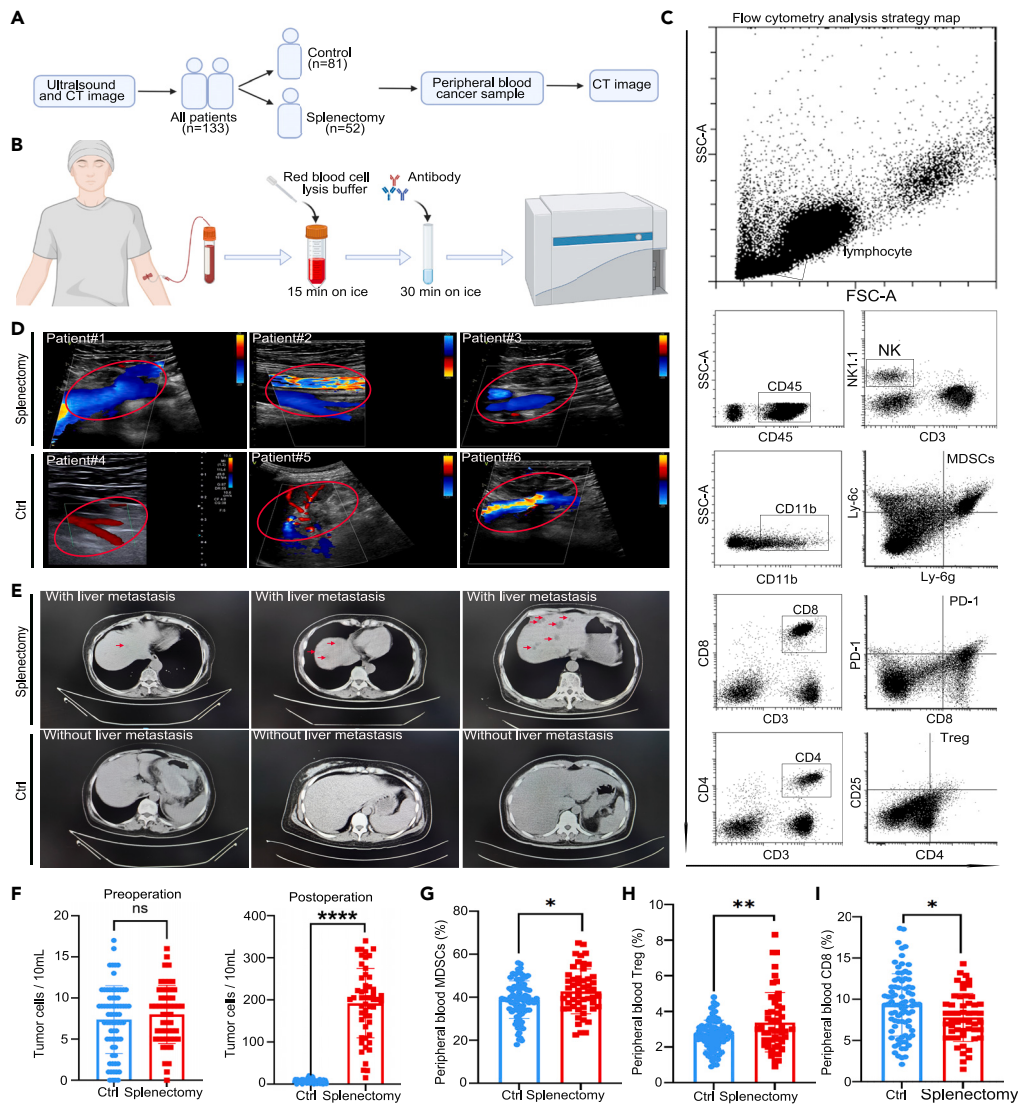https://doi.org/10.1016/j.isci.2024.109045

Figure 1. Immunosuppression occurred in patients with PDAC after combined splenectomy

(A) The experimental grouping and flow chart of 133 patients with pancreatic cancer.

(B) Schematic diagram of peripheral blood collection and flow cytometry detection of patients.

(C) Flow cytometry analysis strategy map of peripheral blood.

(D and E) Abdominal ultrasonography and postoperative abdominal CT observation of postoperative liver metastases in patients with pancreatic cancer, representative images were showed (n = 3 per group).

(F) the detection of circulating tumor cells (CTCs) in peripheral blood of patients with pancreatic cancer.

(G–I) Comparison of MDSCs, Treg and CD8^{+} cell in peripheral blood of patients with spleen deficiency and spleen preservation. statiscally shown with barplot. Student's two-tailed t test was used to determine the significance between two groups. *, p < 0.05; * *, p < 0.01; ***, p < 0.001; ****, p < 0.0001; n. s., no significant statistical difference; the data are presented by mean $\pm$ SD.

RESULTS

Patients with pancreatic cancer with spleen deficiency exhibit tendencies toward immunosuppression, recurrence, and metastasis

To investigate the impact of spleen preservation on postoperative outcomes, we collected data from 133 patients with pancreatic cancer who underwent distal pancreatectomy at Tianjin Medical University Cancer Institute & Hospital from January 2017 to January 2022. Preoperative imaging examination and postoperative histopathology were used to determine lesion location and pathological type. Patients were divided into control group and observation group according to whether they received combined splenectomy, and their imaging data and peripheral blood were obtained. (Figures 1A–1C). No intraoperative deaths occurred in either group. we found that

Table 1. Parameters of patients with pancreatic cancer

Parameters	Groups (n = 133)		
	Control (n = 81)	Splenectomy (n = 52)	p value
Gender			
Male	33 (40.7%)	12 (23.15%)	0.040
Female	48 (59.3%)	40 (66.2%)	
Age (years)	57.41 ± 10.08	53.94 ± 9.31	0.048
Tumor size (cm)	4.25 ± 1.59	4.12 ± 1.80	0.769
TNM			
I	10 (41.7%)	14 (58.3%)	0.137
II	48 (68.6%)	22 (31.4%)	
III	17 (58.6%)	12 (41.4%)	
IV	6 (60.0%)	4 (40.0%)	
MDSCs (%)	40.99 ± 6.89	48.17 ± 9.46	0.024
Treg (%)	2.68 ± 0.99	3.89 ± 1.28	0.007
CD8 (%)	9.96 ± 3.56	7.14 ± 2.64	0.019
High fever	30 (37.0%)	38 (73.1%)	0.000
Infection	5 (6.2%)	11 (21.2%)	0.010
Coagulopathy	6 (7.4%)	10 (19.2%)	0.041
Costs	76349.02 ± 14014.32	89659.59 ± 23455.66	0.000
Stay (days)	9.86 ± 1.79	10.81 ± 2.25	0.000
Death	0	0	–
Metastasis	11 (13.6%)	15 (28.8%)	0.027

Related to Figure 1.
$p < 0.05$: Indicates that the difference is statistically significant.

patients with pancreatic cancer with spleen loss had a higher risk of recurrence and metastasis in postoperative imaging evaluation compared to those with preserved spleen function (Table 1; Figures 1D and 1E). We further analyzed the data of patients who received the same chemotherapy after surgery and obtained similar results (Table 2). These results suggest that spleen loss is associated with postoperative recurrence and metastasis. Our findings indicate that in patients with pancreatic cancer who have undergone splenectomy, more circulating tumor cells (CTCs) can be detected in their peripheral blood compared with pre-operation (Figure 1F). It is inferred that this may be related to the recurrence and metastasis of these patients. In addition, our analysis revealed that the proportion of CD8$^+$ cell in peripheral blood decreased, while the proportion of MDSCs and Treg increased in patients with spleen deficiency (Figure 1G). Patients with spleen deficiency were more likely to experience high fever and infection, and they also had significantly higher hospitalization costs and longer hospital stays compared to patients with preserved spleen function. Furthermore, spleen deficiency was associated with postoperative hypercoagulability. We also collected and tracked 18 patients who underwent distal pancreatic resection with or without splenectomy and the same treatment postoperatively between February 2023 and October 2023 as prospective studies. Compared to patients with preserved spleen, patients with spleen loss have a higher chance of metastasis, and an immunosuppressed state (Table 3).

Splenectomy increases tumor burden and metastasis in pancreatic cancer

Previous studies have shown that splenectomy may increase the number of tumor cells in the blood, reduce the body's ability to fight tumors, and increase the risk of tumor metastasis. To investigate whether spleen loss affects pancreatic cancer progression, we constructed a pancreatic cancer model with splenectomy in mice (Figures 2A–2C). Small animal *in vivo* imaging experiments and statistical analysis of fluorescence values revealed that splenectomized mice had a high burden of pancreatic cancer (Figures 2D and 2E). Meanwhile, more liver metastasis was observed in mice with spleen deficiency (Figure 2F), and liver metastasis were confirmed by Hematoxylin-Eosin staining (Figure 2G). Survival analysis showed that splenectomy shortened the overall survival time of mice (Figure 2H), while tumor volume and weight were increased (Figure 2I). To confirm the effect of splenectomy on survival, we observed the death of tumor-free mice with splenectomy *in vivo*. Our result demonstrated the loss of spleen did not cause death in mice in our experiments (Figure 2J). In addition, *in vivo* experiments with total or partial splenectomy in tumor-bearing mice showed that the increase in the number of CTCs was not associated with the surgical procedure (Figure S1). These results suggest that splenectomy may contribute to tumor burden in mice.

Table 2. Parameters of patients with pancreatic cancer

Parameters	Groups (n = 41)		p value
	Control (n = 18)	Splenectomy (n = 23)	
Gender			
Male	9 (45.0%)	11 (55.0%)	0.890
Female	9 (42.9%)	12 (51.7%)	
Age (years)	56.94 ± 10.33	56.91 ± 8.20	0.991
Tumor size (cm)	4.30 ± 2.27	4.19 ± 2.12	0.854
TNM			
I	6 (35.3%)	11 (64.7%)	0.702
II	8 (50.0%)	22 (50.0%)	
III	3 (60.0%)	2 (40.0%)	
IV	1 (33.3%)	2 (66.7%)	
MDSCs (%)	38.71 ± 6.70	44.67 ± 10.33	0.040
Treg (%)	2.49 ± 0.58	3.46 ± 1.47	0.013
CD8 (%)	9.62 ± 2.72	6.82 ± 2.42	0.001
High fever	6 (25.0%)	18 (75.0%)	0.004
Infection	1 (5.6%)	7 (30.4%)	0.046
Coagulopathy	2 (18.2%)	9 (81.8%)	0.044
Costs	82909.34 ± 21261.34	71693.11 ± 11501.36	0.037
Stay (days)	9.67 ± 1.91	11.26 ± 2.48	0.039
Death	0	0	–
Metastasis	11 (13.6%)	15 (28.8%)	0.027

Related to Figure 1.
$p < 0.05$: Indicates that the difference is statistically significant.

Splenectomy may also reduce the immune clearance of cancer cells by inhibiting the function of the immune system

The spleen has important functions in immunity.[29] Thus, whether splenectomy will further affect the infiltration of immune cells in the tumor. Next, we examined the infiltrating immune cells in the tumor tissue by flow cytometry. Our analysis of immune infiltration in the tumor microenvironment showed that the infiltration ratio of $CD3^+CD4^+$ T lymphocytes, $CD3^+CD8^+$ T lymphocytes, and CD3-NK1.1+ neutral killer cells decreased in mice with spleen loss (Figures 3A–3C). Additionally, there was an increase in Tregs and MDSCs (Figures 3D–3F). Study has found that PD-1 expression can be categorized into three states: PD-1^{high}+CD8$^+$ T, PD-1^{Int}+CD8$^+$ T, and PD-1^{total}+CD8$^+$ T,[30] our results showed that the expression of PD-1^{high}+ CD8+T cell was increased while reducing the level of PD-1^{int}+CD8+T cell in the splenectomy group. These results suggest that spleen loss suppresses immune infiltration in the tumor microenvironment in mice.

High expression of microRNA hsa-7b-5p in pancreatic cancer with splenectomy

In this study, we utilized the GEO database (GSE133589) to identify the 10 most differentially expressed miRNAs in patients with pancreatic cancer with splenectomy (Figure 4A). These miRNAs were found to be associated with the infiltration of immune cells in tumors (Figure 4B). After excluding previously reported miRNAs, we selected the differentially expressed miRNA, hsa-7b-5p, for further analysis (Figure 4C). We found that hsa-7b-5p had a better 5-year risk prediction ability, and its high expression was associated with shorter overall survival time in patients with pancreatic cancer (Figures 4D and 4E). Moreover, miRNA hsa-7b-5p had predictive significance for clinical stage and overall survival of pancreatic cancer (Figures 4F and 4G).

Our analysis showed that the expression of miRNA hsa-7b-5p was higher in T3 and T4 stages than in T1 and T2 stages, and higher in N1 stage than in N0 stage (Figures 4H and 4I). Additionally, compared with stage 1 pathology, miRNA hsa-7b-5p was also highly expressed in stage 2. Further analysis revealed that dead patients with pancreatic cancer expressed higher levels of miRNA hsa-7b-5p than surviving patients (Figures 4J and 4K). We detected a significant increase in the transcription levels of miRNA hsa-7b-5p in the circulating tumor cells of patients with pancreatic cancer after splenectomy, as well as in the *in situ* tumors of mice after splenectomy (Figures 4L and 4M). Similarly, data from the TCGA database showed that it was also associated with pathologic stage and radiotherapy resistance and indicated poor overall survival in patients with pancreatic cancer (Table 4). Therefore, it has the potential to be a predictor of overall survival in patients with pancreatic cancer.

Table 3. Parameters of patients with pancreatic cancer

Parameters	Groups (n = 18)		p value
	Control (n = 11)	Splenectomy (n = 7)	
Gender			
Male	5 (45.5%)	4 (57.1%)	0.629
Female	6 (54.5%)	3 (42.9%)	
Age (years)	57.91 ± 11.84	52.74 ± 8.04	0.325
Tumor size (cm)	4.46 ± 2.55	5.71 ± 2.20	0.302
TNM			
I	4 (36.4%)	2 (28.6%)	0.966
II	4 (36.4%)	3 (42.9%)	
III	1 (18.2%)	1 (14.3%)	
IV	1 (9.1%)	1 (14.3%)	
MDSCs (%)	39.96 ± 4.15	51.81 ± 8.93	0.001
Treg (%)	2.91 ± 0.96	4.16 ± 0.81	0.011
CD8 (%)	9.63 ± 2.75	6.67 ± 1.27	0.017
High fever	4 (36.4%)	6 (85.7%)	0.040
Infection	1 (9.1%)	4 (57.1%)	0.026
Coagulopathy	0 (0.0%)	3 (42.9%)	0.017
Costs	88801.34 ± 23131.13	66733.59 ± 9998.29	0.031
Stay (days)	9.82 ± 1.33	8.29 ± 1.11	0.022
Death	0	0	–
Metastasis	1 (0.0%)	2 (28.6%)	0.060

Related to Figure 1.

$p < 0.05$: Indicates that the difference is statistically significant.

The critical role of microRNA hsa-7b-5p in the remodeling of the immune suppressive environment in pancreatic cancer

We also investigated the relationship between miRNA hsa-7b-5p and immune infiltration of pancreatic cancer. Our results showed that high expression of miRNA hsa-7b-5p was associated with decreased infiltration of T cells, NK cells, and other cytotoxic cells in tumors, while the infiltration of Treg cells increased. These findings suggest that miRNA hsa-7b-5p is associated with the clinical stage and immunosuppression of pancreatic cancer.

To further explore the critical role of miRNA hsa-7b-5p in the remodeling of the immune suppressive environment, we analyzed various sequencing data from multiple databases (ICGC_PAAD_AU_seq, ICGC_PAAD_CA_seq, GSE79668, GSE78229, GSE62452, GSE28735, GSE21501, TCGA_PAAD, GSE57495, GSE71729, E_MTAB_6134, ICGC_PAAD_AU_array) using Spearman's correlation analysis. Our results showed that the expression of miRNA hsa-7b-5p was positively correlated with the infiltration of immunosuppressive cells and the expression of immunosuppressive checkpoints, and negatively correlated with the expression of antigen presenting molecules and immune suppressive chemokines and receptors (Figures 5A and 5B). Therefore, high expression of miRNA hsa-7b-5p indicated resistance to ICB therapy, and led to the remodeling of the immune suppressive environment by increasing the infiltration of immunosuppressive cells and loss of antigen presenting molecules (Figure 5C).

Enhancing immune status by down-regulating microRNA hsa-7b-5p decreases tumor burden and metastasis in pancreatic cancer

In this study, KPC-miRNA HSA-7B-5P-Scramble/sh cell lines with the stable expression of miRNA hsa-7b-5p were constructed, and no differences in their growth were confirmed *in vitro* experiments, and pancreatic cancer models were constructed *in situ* using C57BL/6 mice (Figures 6A, 6B, S2A, and S2B). Our results showed that the tumor growth and metastasis of mice with down-regulated miRNA hsa-7b-5p was significantly inhibited, as confirmed by statistical analysis of tumor volume and metastatic hepatic carcinoma (Figures 6C–6F). To determine whether hsa-7b-5p affects the immune microenvironment of tumors. The infiltration of immune cells in tumor tissues was detected by flow cytometry. Our findings showed that the downregulation of hsa-7b-5p increased the infiltration of CD4 + T cells, CD8$^+$ T cells, and NK + lymphocytes in tumors, while reducing the expression of Treg, PD-1^{high}+CD8$^+$ T cells, and MDSCs (Figures 6G–6L). These results suggest that the down-regulation of miRNA hsa-7b-5p enhances the immune status of pancreatic cancer, leading to reduced tumor burden.
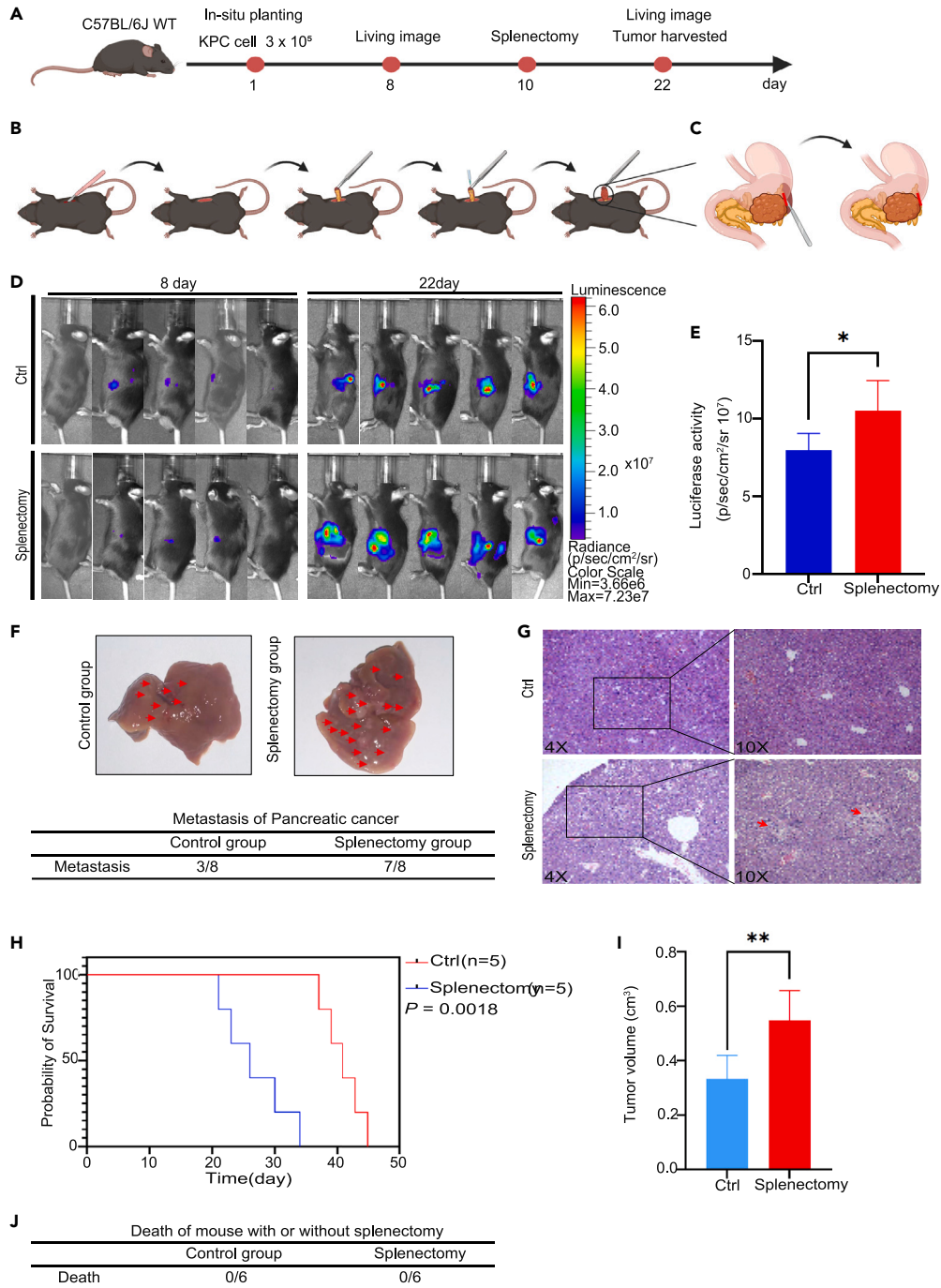
Figure 2. Splenectomy promotes tumor growth and metastasis

(A) The C57BL/6 mice which were orthotopically implanted with KPC cell lines were constructed a splenectomy model with pancreatic cancer.

(B and C) KPC cell line was injected into pancreas tail of mice with splenectomy.

(D and E) The size of pancreatic orthotopic tumors was monitored by small animal *in vivo* imaging technology, and the fluorescence value was calculated at 8 and 22 days.

(F) The numbers of liver metastasis were statistically calculated and displayed with pictures.

(G) Representative images showing liver metastasis by HE staining.

(H and I) The tumor volume and overall survival time were statiscally calculated and shown with barplot. Student's two-tailed t test was used to determine the significance between two groups. *, p < 0.05; * *, p < 0.01; ***, p < 0.001; ****, p < 0.0001; n. s., no significant statistical difference; the data are presented by mean ± SD.

(J) Death of tumor-free mice with or without splenectomy (n = 6 per group). See also Figure S1.
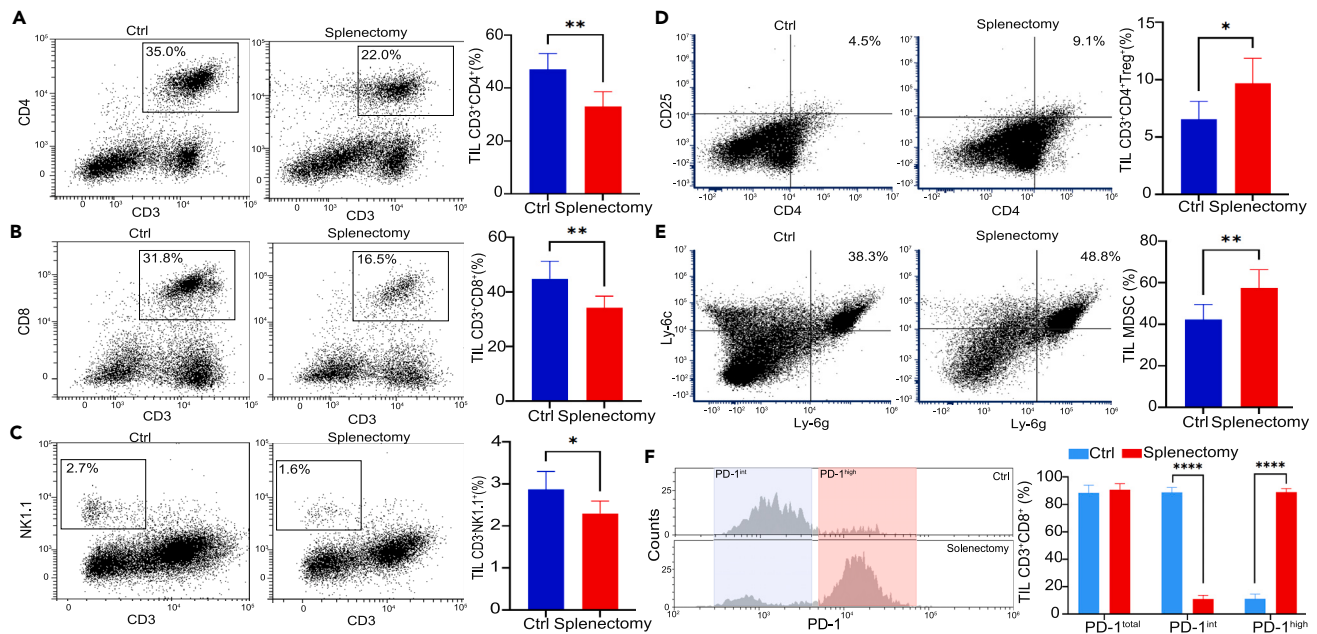
Figure 3. Increased infiltrating inhibitory immune cells in tumor after splenectomy in mice

The murine KPC cell lines were injected orthotopically into C57BL mouse and randomly divided into splenectomy group and non-splenectomy group. The harvested tumors were performed with flow cytometry to detect tumor infiltrating lymphocytes.

(A−F) Representative pictures of Treg cells, MDSCs, CD3+CD4+T cells, CD3-NK1.1 + cells, CD3+CD8+T cells and PD-1+ T cells with different expression states (Left), statistical analysis (Right). Experiments were repeated three times independently. Representative data are shown. Student's two-tailed t test was used to determine the significance between two groups. Data are presented as mean $\pm$ SD. *, $p < 0.05$; **, $p < 0.01$; ***, $p < 0.001$; ****, $p < 0.0001$; n. s., no significant statistical difference.

Overexpression of microRNA hsa-7b-5p increases glycolysis level in pancreatic cancer with TP53 mutation

We performed a pathway enrichment analysis on genes with high expression of miRNA hsa-7b-5p and found that in pancreatic cancer, miRNA hsa-7b-5p was mainly positively correlated with the MAPK signaling pathway, ErbB signaling pathway, and glycolysis-related pathway, while being negatively correlated with the P53 signaling pathway (Figure 7A). We collected a multi-center cohort of patients with pancreatic cancer and found that high expression of miRNA hsa-7b-5p was accompanied by more TP53 mutations, as well as subsequent mutations in genes such as KRAS and CDKN2A (Figure 7B). We aimed to elucidate the potential mechanism of miRNA hsa-7b-5p in increasing tumor burden and accelerating the formation of an immune suppressive environment. Our mRNA sequencing results from the TCGA database revealed that the overexpression of miRNA hsa-7b-5p was positively correlated with the glycolysis process (Figure 7C). Furthermore, our qPCR assay indicated that the elevation of miRNA hsa-7b-5p increased the expression of MCT1, MCT4, GLUT1, GLUT4, and LDHA at mRNA levels (Figure 7D). In conclusion, our study demonstrated that high expression of miRNA hsa-7b-5p can increase tumor burden and promote the formation of an immune suppressive status mainly by elevating glycolysis levels.

Elevation of microRNA hsa-7b-5p is a strong predictor of immune checkpoint blocking treatment efficacy and responsiveness

We aimed to further confirm that high expression of miRNA hsa-7b-5p is a reliable predictor of the efficacy and responsiveness of immunotherapy. To this end, we performed an ROC curve analysis in six different cohort studies, which revealed that high expression of miRNA hsa-7b-5p was associated with a lower response rate to immune checkpoint blocking (ICB) therapy in pancreatic cancer. Specifically, the Ascierto 2016 (36%), Wolf 2021 (36%), and Van 2021 (32%) cohorts demonstrated an average treatment response rate of less than 30% when miRNA hsa-7b-5p was highly expressed, indicating that high expression of miRNA hsa-7b-5p was associated with resistance to anti-PD-1 and PD-L1 therapy (Figures 8A–8C). In our previous study, we observed that the elevation of miRNA hsa-7b-5p in tumors promotes the formation of an immunosuppressive environment. We therefore hypothesized that the expression of miRNA hsa-7b-5p in KPC cells could serve as an effective predictor of anti-PD-1 therapy efficacy.

To test this hypothesis, we conducted experiments using a C57BL/6 mice subcutaneous tumor model (Figure 8D). Our results demonstrated that the tumor size in the KPC-miRNA hsa-7b-5p-sh group significantly decreased following anti-PD-1 treatment, whereas no significant decrease was observed in the KPC-miRNA hsa-7b-5p-scramble group (Figure 8E). We hypothesize that one of the main reasons for inhibiting tumor proliferation was the deficiency of miRNA hsa-7b-5p, which resulted in reduced infiltration of MDSCs and was accompanied by changes in the immune microenvironment combined with anti-PD-1 therapy. To further investigate these changes in the immune
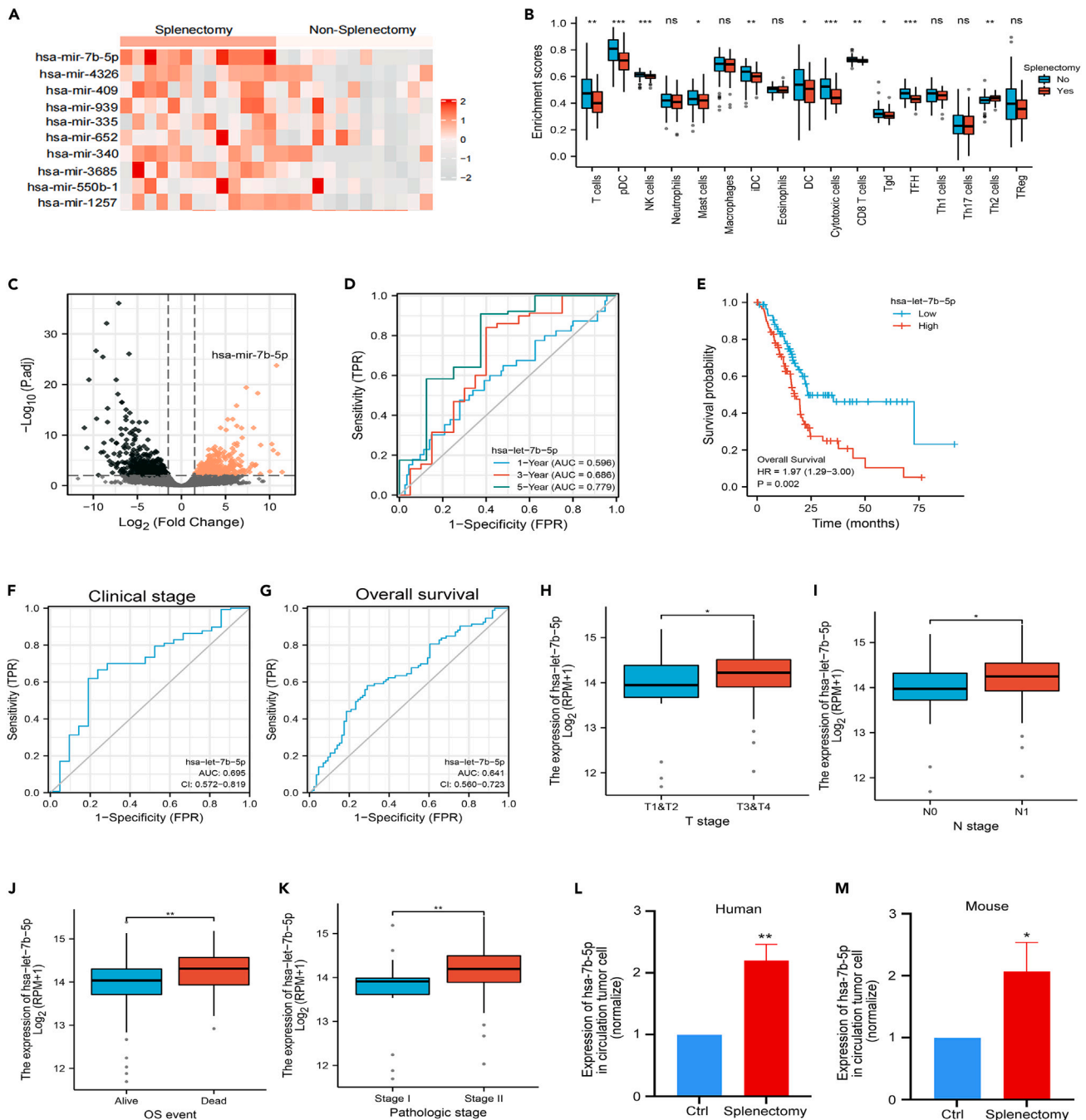
Figure 4. Differential expression and clinical significance of miRNA hsa-7b-5p in pancreatic cancer with splenectomy

(A) Identification of the top 10 differentially expressed miRNAs in patients with pancreatic cancer with splenectomy shown with heatmap.

(B) Association of the differentially expressed miRNAs with immune cell infiltration in tumors using gene set enrichment analysis (GSVA).

(C) Selection of the differentially expressed miRNA, hsa-7b-5p, for further analysis after excluding previously reported miRNAs using the GEO database (GSE133589).

(D) The 5-year risk prediction ability of miRNA hsa-7b-5p in patients with pancreatic cancer with ROC curve.

(E) High expression of miRNA hsa-7b-5p is associated with shorter overall survival time in patients with pancreatic cancer.

(F) Predictive significance of miRNA hsa-7b-5p for clinical stage in patients with pancreatic cancer.

(G) Predictive significance of miRNA hsa-7b-5p for overall survival in patients with pancreatic cancer.

(H) The expression of miRNA hsa-7b-5p in T3 and T4 stages compared to T1 and T2 stages in patients with pancreatic cancer.

(I) The expression of miRNA hsa-7b-5p in N1 stage compared to N0 stage in patients with pancreatic cancer.

Figure 4. *Continued*

(J) The expression of miRNA hsa-7b-5p in deceased patients with pancreatic cancer compared to surviving patients.

(K) The expression of miRNA hsa-7b-5p in stage 2 pathology compared to stage 1 in patients with pancreatic cancer.

(L and M) The transcription levels of miRNA hsa-7b-5p in the circulating tumor cells of patients with pancreatic cancer after splenectomy, as well as in the *in situ* tumors of mice after splenectomy were dectected. Note: The analysis was performed using the GEO database (GSE133589) and statistical analysis including gene set enrichment analysis (GSVA), and survival analysis. Student's two-tailed t test was used to determine the significance between two groups. Data are presented as mean ± SD. *, $p < 0.05$; * *, $p < 0.01$; ***, $p < 0.001$; ****, $p < 0.0001$; n. s., no significant statistical difference.

microenvironment, we used flow cytometry to detect the apoptosis of CD8$^+$ T cells among the four groups. Our results showed that the apoptosis ratio of CD8$^+$ T cells in the KPC-miRNA hsa-7b-5p-sh group was significantly reduced compared to that in the KPC-miRNA hsa-7b-5p-scramble group (Figure 8F). Overall, our findings suggest that the elevated expression of miRNA hsa-7b-5p is a strong predictor of ICB treatment efficacy and responsiveness.

DISCUSSION

Studies have confirmed that defects in spleen function lead to impaired cellular and humoral immunity, making patients prone to adverse reactions such as infection and fever.[31,32] Streptococcus pneumoniae is the most common pathogen.[33] Similarly, infection and fever during

Table 4. Association of hsa-let-7b-5p expression with the clinical features in patients with pancreatic cancer

Characteristics	Low expression of hsa-let-7b-5p (n = 69)	High expression of hsa-let-7b-5p (n = 82)	p value
Pathologic T stage, n (%)			0.003
T1&T2	15 (11.9%)	7 (5.6%)	
T3&T4	54 (37.3%)	75 (45.2%)	
Pathologic N stage, n (%)			0.021
N0	19 (17.2%)	17 (11.5%)	
N1	46 (31.6%)	69 (39.7%)	
Pathologic stage, n (%)			0.002
Stage I	14 (9.9%)	4 (2.3%)	
Stage II&Stage III	52 (40.9%)	76 (46.8%)	
Primary therapy outcome, n (%)			0.314
PD&SD	25 (17.9%)	34 (24.3%)	
PR&CR	42 (30%)	39 (27.9%)	
Residual tumor, n (%)			0.678
R0	44 (32.1%)	49 (32.7%)	
R1&R2	23 (16.4%)	31 (18.8%)	
Histologic grade, n (%)			0.524
G1&G2	47 (33.9%)	54 (37.9%)	
G3&G4	21 (15.3%)	21 (13%)	
Anatomic neoplasm subdivision, n (%)			0.421
Body&Head	52 (41.3%)	62 (44.1%)	
Tail&Other	15 (8.4%)	11 (6.1%)	
Family history of cancer, n (%)			0.679
No	25 (22.5%)	22 (19.8%)	
Yes	35 (31.5%)	29 (26.1%)	
Radiation therapy, n (%)			0.039
No	44 (32.9%)	65 (39.6%)	
Yes	23 (17.7%)	16 (9.8%)	
OS event, n (%)			0.001
Alive	42 (29.6%)	30 (18.4%)	
Dead	21 (20.1%)	51 (31.8%)	

Related to Figure 4.

Chi-square tests and logistic regression models were used. $p < 0.05$: Indicates that the difference is statistically significant.
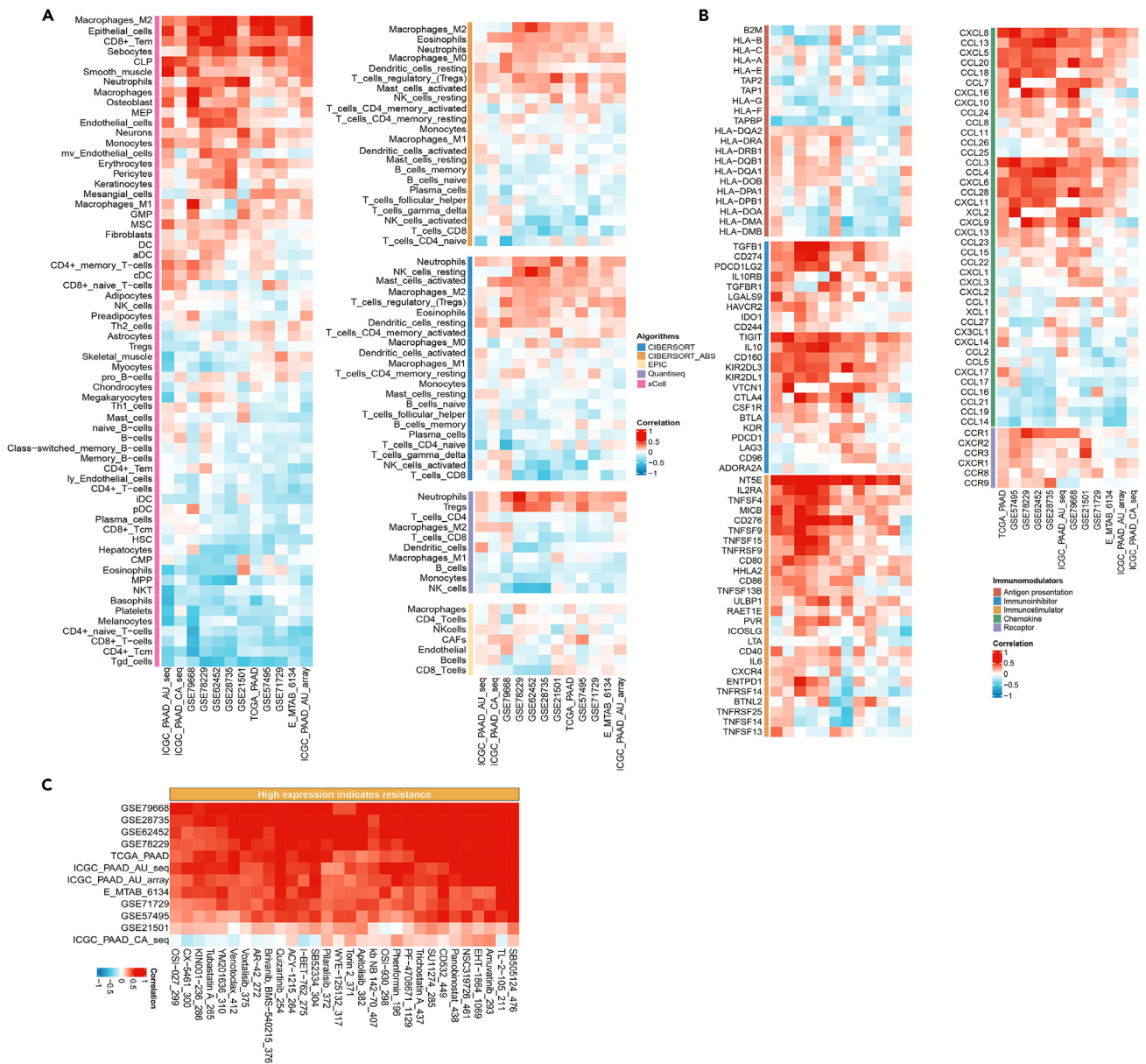
Figure 5. High expression of miRNA hsa-7b-5p reshapes the immunosuppressive environment of pancreatic cancer

(A) The immune infiltration analysis between miRNA hsa-7b-5p and infiltrated immune cells was performed with TCGA and GEO datasets by using Cibersort, Xcell, EPIC, Quantiseq software. Correlation coefficient was displayed with bar plot; (B) the spearman correlation analysis between the expression of miRNA hsa-7b-5p and antigen presentation, immune inhibitor, immune stimulator, chemokine, receptor. Red colored indicated positive correlation; blue colored indicated negative correlation; (C) the estimation of drug sensitivity in patients with high expression of miRNA hsa-7b-5p was conducted among TCGA and GEO datasets.

the resection of patients with distal pancreatic cancer were observed clinically in our study. The spleen serves vital functions in blood filtration and regulation. It plays a critical role in removing aging blood cells, including red blood cells, platelets, and white blood cells, from circulation, while also serving as the primary reservoir for blood cells, such as platelets and white blood cells. However, the number of platelets and white blood cells may increase after splenectomy heightening the risk of blood clot formation. Moreover, the spleen is involved in synthesizing and storing coagulation factor VIII and V, and fibrinogen. Thus, the absence of spleen may lead to a decrease in the levels of these factors, increasing the risk of hypercoagulation.[34,35] Therefore, patients with missing spleens are given more intensive monitoring and care during hospitalization to ensure that infections are controlled and treated in a timely manner. In addition to the cost of the original surgery, additional treatment costs for infections are required. For certain high-risk groups, postoperative infection may lead to more serious consequences, and longer recovery periods and higher costs will be required.
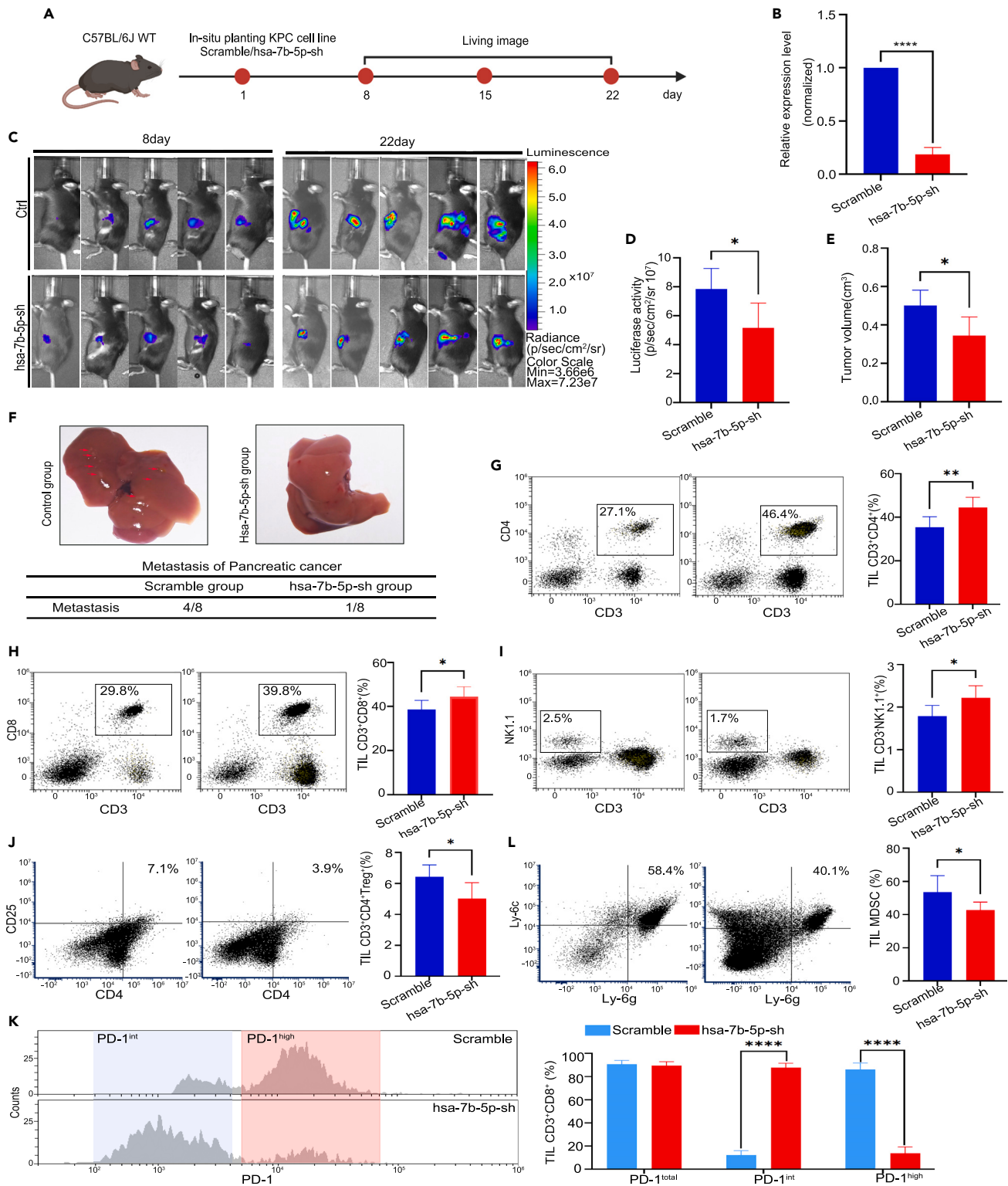
Figure 6. Down-regulating miRNA hsa-7b-5p improve immune state in pancreatic cancer

(A and B) The C57BL/6 mice which were orthotopically implanted with KPC-miR-hsa-7b-5p-Ctrl and KPC-miR-hsa-7b-5p-Sh cell lines were constructed a model with pancreatic cancer.

Figure 6. Continued

(C and D) the size of pancreatic orthotopic tumors was captured by small animal *in vivo* imaging technology, and the BLI fluorescence value was calculated on the 3rd and 20th day.

(E) the tumor volume was statiscally shown with barplot; *, p < 0.05; * *, p < 0.01; ***, p < 0.001; ****, p < 0.0001; n. s., no significant statistical difference; the data are presented by mean + -SD.

(F) The numbers of liver metastasis were statistically calculated and displayed with pictures.

(G–L) The harvested tumors were conducted with flow cytometry to detect tumor infiltrating immune cells. Representative dot plots and statistical analysis of the frequency of tumor-infiltrating T reg cells, MDSCs, CD3+CD4+T cells, CD3-NK1.1+ cells, CD3+CD8+T cells and CD8+PD1+ T cells with different expression states were displayed. Experiments were repeated three times independently. Representative data are shown. Student's two-tailed t test was used to determine the significance between two groups. Data are presented as mean $\pm$ SD. *, p < 0.05; * *, p < 0.01; ***, p < 0.001; ****, p < 0.0001; n. s., no significant statistical difference. See also Figure S2.

The type and stage of cancer determine the relationship between splenectomy and cancer recurrence and metastasis. Splenectomy helps reduce lymphoma recurrence and metastasis. However, for lung or colorectal cancer, splenectomy may have effect on recurrence and metastasis. The spleen has been identified as a major reservoir and source of circulating and tumor-infiltrating immune cells. Circulating and tumor-infiltrating MDSCs and tumor-associated macrophages (TAMs) were increased after splenectomy.[36] Although tumor growth slowed temporarily by splenectomy, it favors cancer lung metastasis and angiogenesis in the long run. And in splenectomy model of liver cancer metastasis suggests that splenectomy promotes liver metastasis by increasing Foxp3 mRNA in the liver.[37] Splenectomy eliminates antitumor effects of streptococcus preparation immunotherapy against mouse liver tumors in a mouse model.[38] Splenectomized patients have significantly increased risk of certain gastrointestinal cancers, other head and neck cancers, and hematologic malignancies, according to Cox proportional hazards regression analysis.[39] In our center's research, we have found that patients with pancreatic cancer who undergo splenectomy have a higher recurrence rate and are more likely to develop liver metastases later, which contributes to disease progression. We aim to further understand the underlying reasons for the impact of splenectomy on the recurrence and metastasis of pancreatic cancer. To achieve this, we will conduct *in vivo* animal experiments to validate and explore our hypothesis. In our experiment, spleen loss not only increased the tumor load of mice, but also reduced the proportion of CD4+ and CD8+ T lymphocytes in the tumor, while increasing the expression of Treg and MDSCs. In addition, according to the different expression states of PD-1, we also obtained that spleen loss increased the expression of PD-1high+CD8+ T cell. The spleen plays an important role in the antitumor immune system by removing tumor cells from the blood, and participates in regulating the response of the body's immune system. Splenectomy affects the function of the body's immune system, which may reduce the body's resistance to tumors and promote tumor growth and spread. We confirmed that splenectomy has been shown to have tumor-promoting and immunosuppressive effects in pancreatic cancer.

Reported studies have demonstrated that splenectomy affects the expression profile of miRNAs, and the regulation of miRNA may be related to physiological processes.[4,40] Thus, we performed miRNA sequencing analysis on the *in situ* tumors of pancreatic cancer after splenectomy and the GEO dataset of splenectomy, aiming to explore the target miRNAs induced by splenectomy-induced alterations. By integrating the differential analysis of sequencing data, we identified miRNA has-7b-5p as the most significantly altered miRNA. Has-let-7b-5p, a crucial miRNA, exhibits diverse functions and potential clinical applications. In acute myeloid leukemia (AML), downregulation of has-let-7b-5p is associated with increased FTO levels and promotes AML cell proliferation through the m6A/MYC signaling pathway.[24] Furthermore, has-let-7b-5p plays a significant role in non-small cell lung cancer (NSCLC). It binds to Hsa-miR-184 in plasma-derived exosomes and Hsa-miR-22-3p in circulating miRNAs, which are involved in WNT/β-catenin and mTOR/AKT signaling pathways and associated with tumor treatment resistance.[25,26] In glioblastoma, has-let-7b-5p has been identified as a key miRNA regulating candidate genes and critical processes such as migration, invasion, and the cell cycle.[27] Additionally, high expression of has-let-7b-5p is correlated with endoplasmic reticulum stress, inflammatory response, and apoptosis in acute PE. This indicates the involvement of has-let-7b-5p in the pathogenesis of PE and its potential as an indicator for treatment and prognosis evaluation.[28] In pancreatic cancer, miR-7b-5p has been shown to regulate multiple oncogenic pathways, including the EGFR/PI3K/Akt signaling pathway and the Raf/MEK/ERK pathway. Overall, the available evidence suggests that miR-7b-5p plays an important role in tumorigenesis and may represent a promising target for cancer therapy. We found that miRNA hsa-7b-5p has superior 5-year risk prediction ability and its high expression is associated with poor overall survival in patients with pancreatic cancer. In addition, miRNA hsa-7b-5p has predictive significance in clinical stage and overall survival of pancreatic cancer. Specifically, the expression of miRNA hsa-7b-5p is higher in T3 and T4 stages and N1 stage, and in dead patients compared to surviving patients. Our study also revealed that miRNA hsa-7b-5p plays a critical role in the remodeling of the immune suppressive environment, where its expression is positively correlated with immunosuppressive cells and checkpoints and negatively correlated with antigen presenting molecules and immune suppressive chemokines and receptors. Furthermore, our findings demonstrated that high expression of miRNA hsa-7b-5p indicates resistance to immune checkpoint blockade (ICB) therapy. We also established a KPC-miRNA hsa-7b-5p-scramble/sh cell line to confirm the impact of miRNA hsa-7b-5p expression on pancreatic cancer growth in a mouse model. The results showed that miRNA hsa-7b-5p down-regulation reduced the infiltration of CD4+ T cells, CD8+ T cells, and NK + lymphocytes in tumors and inhibited tumor growth. Pathway enrichment analysis showed that miRNA hsa-7b-5p is positively correlated with MAPK signaling pathway, ErbB signaling pathway, and Glycolysis-related pathway, but negatively correlated with P53 signaling pathway. Moreover, miRNA hsa-7b-5p overexpression was associated with TP53 mutation and subsequent mutations in genes such as KRAS and CDKN2A, which promote glycolysis. We also demonstrated that high expression of miRNA hsa-7b-5p results in resistance to anti-PD-1 and PDL1 therapy in pancreatic cancer. In a subcutaneous tumor model, anti-PD-1 treatment significantly reduced tumor size in the KPC-miRNA hsa-7b-5p-sh group, but not in the KPC-miRNA hsa-7b-5p-scramble group. Additionally, the
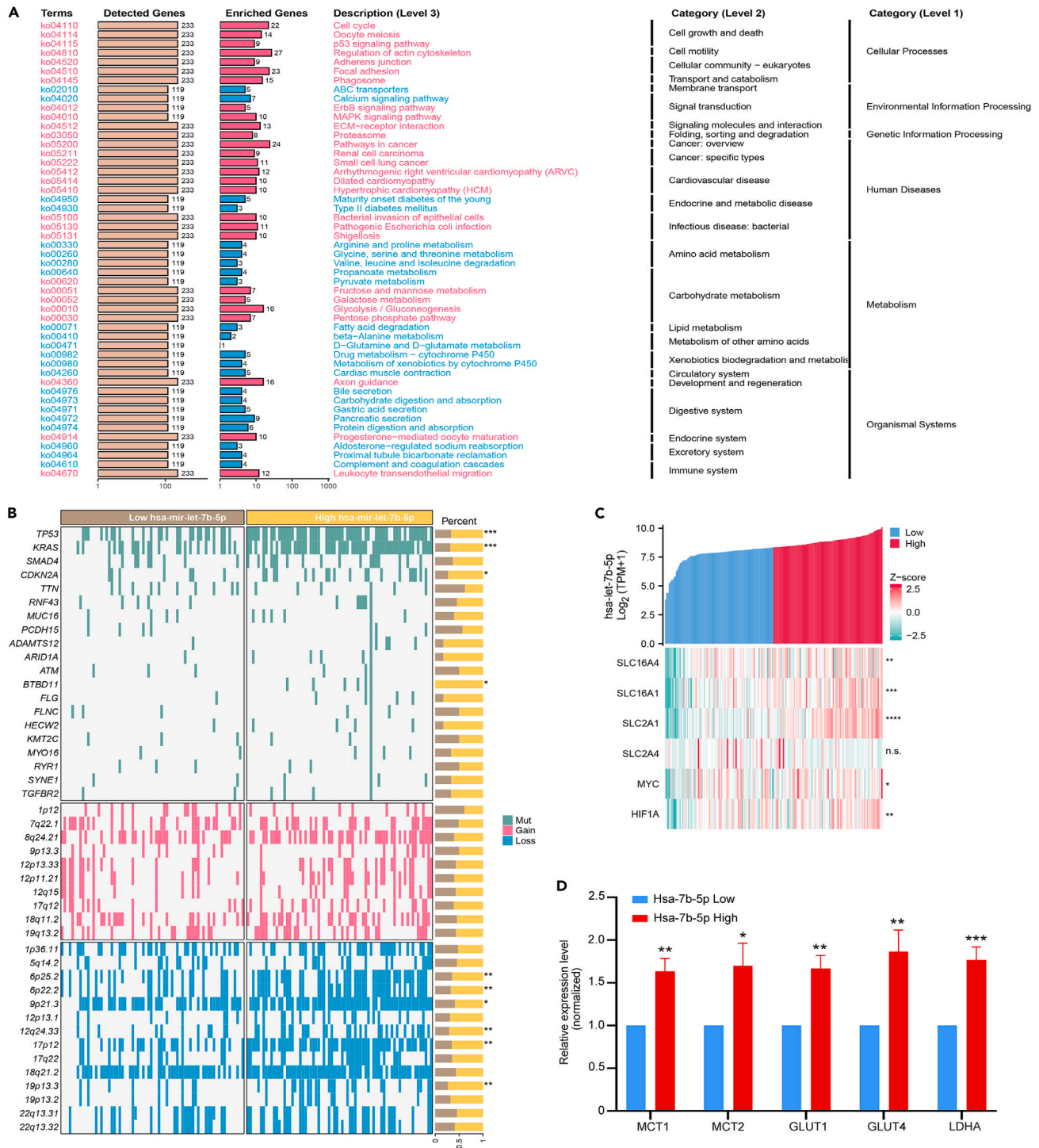
Figure 7. Overexpression of miRNA hsa-7b-5p increases glycolysis level in pancreatic cancer with TP53 mutation

(A) The KEGG analysis was conducted for further validating the function of miRNA hsa-7b-5p; the red colored indicated upregulated pathways, and the blue colored indicated down regulated pathways; the significantly differentially expressed genes were filtered based on the logFC, and the adj. p_value <0.05 was considered to represent a significant difference.

(B) we observed the all-mutation sites in patients with pancreatic cancer from TCGA database between high expression of miRNA hsa-7b-5p group and low expression of miRNA hsa-7b-5p group; the ratio of mutation status in two groups was calculated.

Figure 7. Continued

(C) the sperman's correlation analysis between the remarkable genes which were correlated positively with glycolytic process and miRNA hsa-7b-5p was conducted and shown with co-expressed heatmap.

(D) QPCR assay was conducted to estimate the relationship between miRNA hsa-7b-5p and metabolic markers (MCT1, MCT4, GLUT1 and GLUT4). Experiments were repeated three times independently. *, Student's two-tailed t test was used to determine the significance between two groups. $p < 0.05$; * *, $p < 0.01$; ***, $p < 0.001$; ****, $p < 0.0001$; n. s., no significant statistical difference.

apoptosis ratio of CD8^{+} T cells in the KPC-miRNA hsa-7b-5p-sh group was significantly reduced compared to the KPC-miRNA hsa-7b-5p-scramble group. These results suggest that miRNA hsa-7b-5p may serve as a potential prognostic biomarker and therapeutic target in pancreatic cancer.

The core findings of this study suggest that miRNA hsa-7b-5p is a key player in the pathogenesis of pancreatic cancer and may serve as a promising prognostic biomarker and therapeutic target. The study reveals that miRNA hsa-7b-5p is significantly altered after splenectomy-induced alterations, and its dysregulation is associated with poor overall survival and resistance to immune checkpoint blockade therapy. In the future, further studies are needed to investigate the mechanisms underlying miRNA hsa-7b-5p dysregulation and its effects on tumorigenesis and immune evasion in pancreatic cancer. Additionally, studies could explore the therapeutic potential of targeting miRNA hsa-7b-5p in combination with other therapies, such as immune checkpoint blockade or glycolysis inhibitors. The findings of this study may have significant implications for the development of personalized cancer therapies and the identification of new prognostic biomarkers.

Conclusion

In summary, this study identified miRNA hsa-7b-5p as a promising prognostic biomarker and therapeutic target for pancreatic cancer. The expression of miRNA hsa-7b-5p is associated with poor overall survival and resistance to immune checkpoint blockade therapy. Moreover, miRNAhsa-7b-5p plays a critical role in the remodeling of the immune suppressive environment and promotes tumorigenesis through various oncogenic pathways. The results of this study have significant implications for the development of personalized therapies for patients with pancreatic cancer. Further research is warranted to elucidate the underlying mechanisms of miRNAhsa-7b-5p in pancreatic cancer and explore its potential as a diagnostic and prognostic biomarker.

Limitation of the study

In summary, potential limitations of this study include sample selection bias due to the reliance on data from a single center, the limited generalizability of findings from mouse models to human contexts, and the intricate nature of miRNA functionality, warranting further in-depth research into its mechanisms of action.

STAR★METHODS

Detailed methods are provided in the online version of this paper and include the following:

- KEY RESOURCES TABLE
- RESOURCE AVAILABILITY
  - Lead contact
  - Materials availability
  - Data and code availability
- METHOD DETAILS
  - Patient data collection
  - C57BL/6J mice
  - Mouse model
  - Sequencing data acquisition and preprocessing
  - Identification of differentially expressed genes (DEGs)
  - Gene ontology (GO) and kyoto encyclopedia of genes and genomes (KEGG) pathway enrichment analysis
  - Risk factor estimation
  - Immune infiltration analysis
  - The analysis of tumor burden in pancreatic cancer
  - Cell culture
  - The detection of CTCs
  - Living image
  - Flow cytometry analysis
  - RNA isolation and quantitative real-time PCR
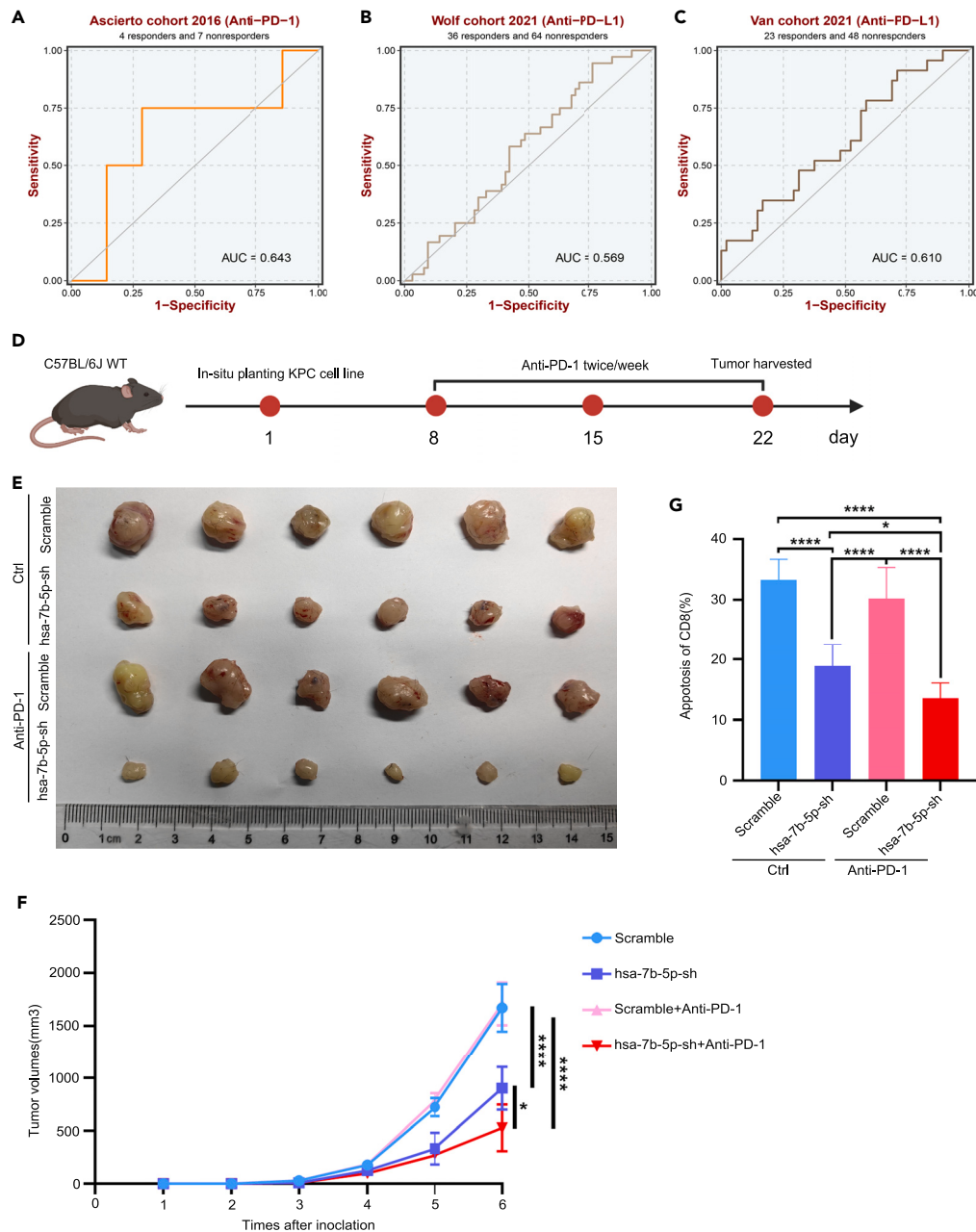 - *In vivo* anti-PD-1 therapy
  - Statistical analysis

Figure 8. Hsa-miR-7b-5p knockdown improves anti-PD-1 therapy

(A–C) The ROC analysis was performed and AUC value was calculated in anti-PD1 therapy cohorts according to the expression of miRNA hsa-7b-5p; (D) KPC-miRNA hsa-7b-5p-scramble/sh cell lines were implanted subcutaneously in C57BL/6 immunocompetent mice, the blocking antibody of PD1 was used for intraperitoneal injection (red dots represented the beginning of administration); three times a week until the tumor harvested.

(E–G) The tumor size of pancreatic cancer was calculated among four groups, and shown with bar plot; the data were statistically analyzed by histogram; the mean +SD was used for statistical analysis between groups, * *, p < 0.01; *, p < 0.05; * **, p < 0.001; n. s., no significant statistical difference.

SUPPLEMENTAL INFORMATION

Supplemental information can be found online at https://doi.org/10.1016/j.isci.2024.109045.

ACKNOWLEDGMENTS

AUTHOR CONTRIBUTIONS

DECLARATION OF INTERESTS

REFERENCES

1. Siegel, R.L., Miller, K.D., Fuchs, H.E., and Jemal, A. (2021). Cancer Statistics, 2021. CA. Cancer J. Clin. 71, 7–33. https://doi.org/10.3322/caac.21654.

2. Rawla, P., Sunkara, T., and Gaduputi, V. (2019). Epidemiology of Pancreatic Cancer: Global Trends, Etiology and Risk Factors. World J. Oncol. 10, 10–27. https://doi.org/10.14740/wjon1166.

3. Schwartz, P.E., Sterioff, S., Mucha, P., Melton, L.J., and Offord, K.P. (1982). Postsplenectomy Sepsis and Mortality in Adults. JAMA 248, 2279–2283.

4. Dragomir, M., Petrescu, D.G.E., Manga, G.E., Călin, G.A., and Vasilescu, C. (2016). Patients After Splenectomy: Old Risks and New Perspectives. Chirurgia 111, 393–399. https://doi.org/10.21614/chirurgia.111.5.393.

5. Du, T., and Zamore, P.D. (2005). microPrimer: the biogenesis and function of microRNA. Development 132, 4645–4652. https://doi.org/10.1242/dev.02070.

6. Bartel, D.P. (2009). MicroRNAs: Target Recognition and Regulatory Functions. Cell 136, 215–233. https://doi.org/10.1016/j.cell.2009.01.002.

7. Ha, M., and Kim, V.N. (2014). Regulation of microRNA biogenesis. Nat. Rev. Mol. Cell Biol. 15, 509–524. https://doi.org/10.1038/nrm3838.

8. Lee, Y.S., and Dutta, A. (2009). MicroRNAs in Cancer. Annu. Rev. Pathol. 4, 199–227. https://doi.org/10.1146/annurev.pathol.4.110807.092222.

9. Mohr, A.M., and Mott, J.L. (2015). Overview of MicroRNA Biology. Semin. Liver Dis. 35, 3–11. https://doi.org/10.1055/s-0034-1397344.

10. Pauley, K.M., Cha, S., and Chan, E.K.L. (2009). MicroRNA in autoimmunity and autoimmune diseases. J. Autoimmun. 32, 189–194. https://doi.org/10.1016/j.jaut.2009.02.012.

11. James, J.P., Riis, L.B., Malham, M., Høgdall, E., Langholz, E., and Nielsen, B.S. (2020). MicroRNA Biomarkers in IBD—Differential Diagnosis and Prediction of Colitis-Associated Cancer. Int. J. Mol. Sci. 21, 7893. https://doi.org/10.3390/ijms21217893.

12. Bocchetti, M., Ferraro, M.G., Ricciardiello, F., Ottaiano, A., Luce, A., Cossu, A.M., Scrima, M., Leung, W.-Y., Abate, M., Stiuso, P., et al. (2021). The Role of microRNAs in Development of Colitis-Associated Colorectal Cancer. Int. J. Mol. Sci. 22, 3967. https://doi.org/10.3390/ijms22083967.

13. Zhang, X., Mao, H., and Lv, Z. (2013). MicroRNA role in thyroid cancer pathogenesis. Front. Biosci. 18, 734–739. https://doi.org/10.2741/4135.

14. Bagnyukova, T.V., Pogribny, I.P., and Chekhun, V.F. (2006). MicroRNAs in normal and cancer cells: a new class of gene expression regulators. Exp. Oncol. 28, 263–269.

15. Svoronos, A.A., Engelman, D.M., and Slack, F.J. (2016). OncomiR or Tumor Suppressor? The Duplicity of MicroRNAs in Cancer. Cancer Res. 76, 3666–3670. https://doi.org/10.1158/0008-5472.can-16-0359.

16. Grimes, J.A., Prasad, N., Levy, S., Cattley, R., Lindley, S., Boothe, H.W., Henderson, R.A., and Smith, B.F. (2016). A comparison of microRNA expression profiles from splenic hemangiosarcoma, splenic nodular hyperplasia, and normal spleens of dogs. BMC Vet. Res. 12, 272. https://doi.org/10.1186/s12917-016-0903-5.

17. Yi, Z., Fu, Y., Ji, R., Li, R., and Guan, Z. (2012). Altered microRNA Signatures in Sputum of Patients with Active Pulmonary Tuberculosis. PLoS One 7, e43184. https://doi.org/10.1371/journal.pone.0043184.

18. Staedel, C., and Darfeuille, F. (2013). MicroRNAs and bacterial infection. Cell Microbiol. 15, 1496–1507. https://doi.org/10.1111/cmi.12159.

19. Abdalla, A.E., Duan, X., Deng, W., Zeng, J., and Xie, J. (2016). MicroRNAs play big roles in modulating macrophages response toward mycobacteria infection. Infect. Genet. Evol. 45, 378–382. https://doi.org/10.1016/j.meegid.2016.09.023.

20. Ji, H., Fan, L., Shan, A., Wang, W., Ning, G., Cao, Y., and Jiang, X. (2022). Let7b-5p inhibits insulin secretion and decreases pancreatic β-cell mass in mice. Mol. Cell. Endocrinol. 540, 111506. https://doi.org/10.1016/j.mce.2021.111506.

21. Latini, A., Vancheri, C., Amati, F., Morini, E., Grelli, S., Matteucci, C., Petrone, V., Colona, V.L., Murdocca, M., Andreoni, M., et al. (2022). Expression analysis of miRNA hsa-let7b-5p in naso-oropharyngeal swabs of COVID-19 patients supports its role in regulating ACE2 and DPP4 receptors. J. Cell Mol. Med. 26, 4940–4948. https://doi.org/10.1111/jcmm.17492.

22. Xue, F., Feng, H., Wang, T., Feng, G., Ni, N., Wang, R., and Yuan, H. (2023). hsa_circ_0000264 promotes tumor progression via the hsa-let-7b-5p/HMGA2 axis in head and neck squamous cell carcinoma. Oral Dis. 29, 2677–2688. https://doi.org/10.1111/odi.14399.

23. Chen, G., and Yan, J. (2022). Dysregulation of SNHG16(lncRNA)-Hsa-Let-7b-5p(miRNA)-TUBB4A (mRNA) Pathway Fuels Progression of Skin Cutaneous Melanoma. Curr. Protein Pept. Sci. 23, 791–809. https://doi.org/10.2174/1389201023666220928120902.

24. Zhou, Y.-L., Xu, Z.-J., Zhou, J.-D., Zhang, T.-J., Yao, D.-M., Ma, J.-C., Lin, J., and Qian, J. (2021). [Overexpression of LncRNA ITGB2-AS1 Predicts Adverse Prognosis in Acute Myeloid Leukemia. Zhongguo shi yan xue ye xue za zhi 29, 1436–1449. https://doi.org/10.19746/j.cnki.issn.1009-2137.2021.05.011.

25. Vadla, G.P., Daghat, B., Patterson, N., Ahmad, V., Perez, G., Garcia, A., Manjunath, Y., Kaifi, J.T., Li, G., and Chabu, C.Y. (2022). Combining plasma extracellular vesicle Let-7b-5p, miR-184 and circulating miR-22-3p levels for NSCLC diagnosis and drug resistance prediction. Sci. Rep. 12, 6693. https://doi.org/10.1038/s41598-022-10598-x.

26. Zhu, X.-D., Fan, Y.-F., Zhao, Y., Song, X.-Y., Liu, X.-S., Gao, Z.-J., and Yuan, K. (2023). Thymidine Kinase 1 as a target is regulated by the hsa-let-7b-5p/LINC00665 axis and affects NSCLC prognosis. Heliyon 9, e21328. https://doi.org/10.1016/j.heliyon.2023.e21328.

27. Xi, X., Chu, Y., Liu, N., Wang, Q., Yin, Z., Lu, Y., and Chen, Y. (2019). Joint bioinformatics analysis of underlying potential functions of hsa-let-7b-5p and core genes in human glioma. J. Transl. Med. 17, 129. https://doi.org/10.1186/s12967-019-1882-7.

28. Liu, T.W., Liu, F., and Kang, J. (2020). Let-7b-5p is involved in the response of endoplasmic reticulum stress in acute pulmonary embolism through upregulating the expression of stress-associated endoplasmic reticulum protein 1. IUBMB Life 72, 1725–1736. https://doi.org/10.1002/iub.2306.

29. Brendolan, A., Rosado, M.M., Carsetti, R., Selleri, L., and Dear, T.N. (2007). Development and function of the mammalian spleen. Bioessays 29, 166–177. https://doi.org/10.1002/bies.20528.

30. Liu, J., Jiang, W., Zhao, K., Wang, H., Zhou, T., Bai, W., Wang, X., Zhao, T., Huang, C., Gao, S., et al. (2019). Tumoral EHF predicts the efficacy of anti-PD1 therapy in pancreatic ductal adenocarcinoma. J. Exp. Med. 216, 656–673. https://doi.org/10.1084/jem.20180749.

31. Arnott, A., Jones, P., Franklin, L.J., Spelman, D., Leder, K., and Cheng, A.C. (2018). A Registry for

Patients With Asplenia/Hyposplenism Reduces the Risk of Infections With Encapsulated Organisms. Clin. Infect. Dis. *67*, 557–561. https://doi.org/10.1093/cid/ciy141.

32. Di Sabatino, A., Carsetti, R., and Corazza, G.R. (2011). Post-splenectomy and hyposplenic states. Lancet *378*, 86–97. https://doi.org/10.1016/s0140-6736(10)61493-6.

33. Tahir, F., Ahmed, J., and Malik, F. (2020). Post-splenectomy Sepsis: A Review of the Literature. Cureus *12*, e6898. https://doi.org/10.7759/cureus.6898.

34. Crary, S.E., and Buchanan, G.R. (2009). Vascular complications after splenectomy for hematologic disorders. Blood *114*, 2861–2868. https://doi.org/10.1182/blood-2009-04-210112.

35. Mohren, M., Markmann, I., Dworschak, U., Franke, A., Maas, C., Mewes, S., Weiss, G., and Jentsch-Ullrich, K. (2004). Thromboembolic complications after splenectomy for hematologic diseases. Am. J. Hematol. *76*, 143–147. https://doi.org/10.1002/ajh.20018.

36. Sevmis, M., Yoyen-Ermis, D., Aydin, C., Bilgic, E., Korkusuz, P., Uner, A., Hamaloglu, E., Esendagli, G., and Karakoc, D. (2017). Splenectomy-Induced Leukocytosis Promotes Intratumoral Accumulation of Myeloid-Derived Suppressor Cells, Angiogenesis and Metastasis. Immunol. Invest. *46*, 663–676. https://doi.org/10.1080/08820139.2017.1360339.

37. Higashijima, J., Shimada, M., Chikakiyo, M., Miyatani, T., Yoshikawa, K., Nishioka, M., Iwata, T., and Kurita, N. (2009). Effect of splenectomy on antitumor immune system in mice. Anticancer Res. *29*, 385–393.

38. Imai, S., Nio, Y., Shiraishi, T., Tsubono, M., Morimoto, H., Tseng, C.C., Kawabata, K., Masai, Y., and Tobe, T. (1991). Splenectomy abolishes antitumor effect of immunotherapy with streptococcal preparation, OK-432, on mouse liver tumors. Anticancer Res. *11*, 1269–1274.

39. Sun, L.-M., Chen, H.-J., Jeng, L.-B., Li, T.-C., Wu, S.-C., and Kao, C.-H. (2015). Splenectomy and increased subsequent cancer risk: a nationwide population-based cohort study. Am. J. Surg. *210*, 243–251. https://doi.org/10.1016/j.amjsurg.2015.01.017.

40. Dragomir, M.P., Tudor, S., Okubo, K., Shimizu, M., Chen, M., Giza, D.E., He, W.R., Ivan, C., Calin, G.A., and Vasilescu, C. (2019). The non-coding RNome after splenectomy. J. Cell Mol. Med. *23*, 7844–7858. https://doi.org/10.1111/jcmm.14664.

STAR★METHODS

KEY RESOURCES TABLE

REAGENT or RESOURCE	SOURCE	IDENTIFIER
Antibodies		
APC/Fire™ 750 anti-mouse CD45	Biolegend	103154; RRID: AB_2572116j
APC anti-mouse CD3	Biolegend	100236; RRID: AB_2561456
Brilliant Violet 421™ anti-mouse CD4	Biolegend	100544; RRID: AB_11219790
FITC anti-mouse CD8a	Biolegend	100706; RRID: AB_312745
Brilliant Violet 605™ anti-mouse CD279 (PD-1)	Biolegend	135219; RRID: AB_11125371R
Brilliant Violet 785™ anti-mouse NK-1.1	Biolegend	108749; RRID: AB_2564304R
Biological samples		
Human peripheral blood	The study cohort was inpatients from the Department of Pancreatic cancer of Tianjin Medical University Cancer Institute & Hospital	N/A
Experimental models: Cell lines		
KPC	This paper	N/A
Experimental models: Organisms/strains		
Mouse:C57BL/6J	This paper	N/A
Oligonucleotides		
Primers used in study. See Table S1	This paper	N/A
Kras-Forward: GTCTTTCCCCAG CAC AGTGC	This paper	N/A
Kras-Reverse: CTCTTGCCTACGCCA CCAGCTC	This paper	N/A
Trp53-Forward: AGCCTGCCTAGCTTCCTCAGG	This paper	N/A
Trp53-Reverse: CTTGGAGACATAGCCACACTG	This paper	N/A
MCT1-Forward: GTGAGGAAGGAAGGATTGAGGAA	This paper	N/A
MCT1-Revese: CGAGCACGACAAGAAACAGATA AG	This paper	N/A
MCT2-Forward: ACCCATGGCATGAGTGATGAG	This paper	N/A
MCT2-Reverse: TCAGTCCAGA TCCTTGTGTCAGA	This paper	N/A
GLUT1-Forward: TCCAGACGAACCTGGAAG	This paper	N/A
GLUT1- Reverse: AGTCCATCTGTCCTGGTGA	This paper	N/A
GLUT2-Forward: GTTGGAAGAGGAAGTCAGGGCA	This paper	N/A
GLUT2-Reverse: TCACGGAGACCTTCTGCTCAG	This paper	N/A
LDHA-Forward: ACGCAGACAAG GAGCAGTGGAA	This paper	N/A
LDHA-Reverse: TGCTCTCAGCCAAGTCTGCCA	This paper	N/A

Continued

REAGENT or RESOURCE	SOURCE	IDENTIFIER
Software and algorithms		
GraphPad Prism 9.0	GraphPad Software	https://www.graphpad.com/
CytoExpert 5.7.3	Beckman Coulter	https://resources.mybeckman.cn/
Adobe Illustrator	Adobe	https://www.adobe.com/

RESOURCE AVAILABILITY

Lead contact

Further information and requests for resources and reagents should be directed to and will be fulfilled by the Lead Contact, Xiaona Wang (wangxiaona0520@126.com).

Materials availability

This study did not generate new unique reagents.

Data and code availability

- All data reported in this paper can be made available by lead contact upon request.
- This paper does not report original code.
- Any additional information required to reanalyze the data reported in this paper is available from the lead contact upon request.

METHOD DETAILS

Patient data collection

A total of 149 patients with remote pancreatic cancer and data from the Department of Pancreatic Oncology, Tianjin Medical University Cancer Institute & Hospital. It was approved by Ethics Committee and Institutional Review Committee of Cancer Hospital and Research Institute of Tianjin Medical University.

C57BL/6J mice

C57BL/6J mice aged 4 to 6 weeks were purchased from Beijing Spifu Company and raised in a clean room with room temperature of about $20^{\circ}C$ and humidity of 50% to 60%, providing high-quality feed and drinking water. All animal experiments were performed according to protocols approved by the Ethics Committee and Institutional Review Board of Tianjin Medical University Cancer Institute & Hospital (NSFC-AE-2022161).

Mouse model

For *in situ* tumor model, 1×106 luciferase labeled KPC cells were re-suspended in 40 µl PBS buffer containing 50% matrix gel, and then injected *in situ* into the pancreatic tail of C57BL/6J mice aged 4-6 weeks. Saline was used to clean the injection site to see if cell suspension leakage or bleeding occurred, then the pancreas was returned to the peritoneal cavity, the abdominal wall and skin were closed with sutures, and mice with cell suspension leakage were excluded. For the splenectomy model, the splenic arteriovenous vein was identified in the splenic hilum and tail of pancreas, the spleen was resected after the splenic arteriovenous ligation, and the abdominal wall and skin were sutured.

Sequencing data acquisition and preprocessing

We obtained mRNA expression data and corresponding phenotypic data of 178 pancreatic cancer specimens from The Cancer Genome Atlas (TCGA) database. Data preprocessing was performed by transforming gene expression values using log2 (normalized RSEM count 1) and removing genes with low or no expression (genes with an average count greater than 1 and expressed in more than 75% of patients). Relative expression (RLE) and standardized scale-free standard error (NUSE) were provided using the affyPLM package. The original gene expression data was background corrected using the robust multi-array averaging (RMA), standardized using the quantitative method, and summarized using the topic polishing method. To ensure the accuracy of our analysis, we used multiple probes to match genes and set the average expression value as the relative expression value. We obtained genes related to cell biology from the human molecular feature database v7.2 (MSigDB). Additionally, we validated characteristic genes in pancreatic cancer patients from both TCGA and Gene Expression Omnibus (GEO) databases. We determined differentially expressed genes using a Bayesian test (FDR < 0.05) and analyzed immune infiltration from various GEO datasets, including GSE79668, GSE28735, GSE62452, GSE78229, GSE71729, GSE57495, GSE21501, and E_MATB_6134. The MSigDB database provided a number of gene sets based on factors such as position, function, metabolic pathways, and target binding, and we used this to create gene sets composed of similar location or function of multiple genes, stored in the MSigDB data.

Identification of differentially expressed genes (DEGs)

To identify differentially expressed genes (DEGs), we used the limma package to conduct differential expression analysis on both TCGA and GEO datasets. Volcano plots were used to visually display the mRNA sequencing results of the DEGs, and the Venn diagram was drawn using the ggplot2 package. Genes with an adjusted p-value less than 0.05 were considered to be statistically significant.

Gene ontology (GO) and kyoto encyclopedia of genes and genomes (KEGG) pathway enrichment analysis

GO functional enrichment analysis is a commonly used method for large-scale functional enrichment of genes, which consists of three main parts: biological process (BP), molecular function (MF), and cellular component (CC). The KEGG database is a widely used database for storing information about genomes, biological pathways, diseases, and drugs. To perform GO and KEGG pathway enrichment analysis, we used the clusterProfile package. We considered adj.p value less than 0.05 to be statistically significant. The DEGs were subjected to KEEG/GO pathway enrichment analysis, and the results were further presented using a histogram and a bubble plot. The bubble plot depicts different ratios in their respective pathways, and different gradient colors represent different adj.P values < 0.05, while different circle sizes represent the count of genes.

Risk factor estimation

We employed time-dependent receiver operating characteristic (ROC) curve analysis to evaluate the performance of our risk model. We calculated the sensitivity and specificity of predicting the survival rate of triple-negative breast cancer during 1-, 3-, and 5-year follow-up periods. Additionally, we examined the association between the risk score and other clinical indicators such as age, gender, TNM stage, and histological grade. Using a point map, we displayed the distribution of patient death events based on the increase of risk score values. We utilized a heatmap to visualize the expression distribution of each characteristic gene in two different risk groups. To assess the independence and reliability of our prognostic model, we included commonly used indicators such as age, TNM stage, and histological grade to predict the prognosis of pancreatic cancer. We performed univariate and multivariate Cox regression analyses with the clinical characteristics and risk scores of PDAC patients in the TCGA cohort to determine the clinical factors associated with survival. We further verified whether the targeted gene was related to other survival-related clinical information using a log-rank test.

Immune infiltration analysis

We employed CIBERSORT, EPIC, Xcell, Quantiseq, and CIBERSORT_ABS to detect the infiltration of immune cells with RNA-Seq expression profile data in tumor tissues. CIBERSORT provides a gene signature of 24 immune cells, including B cells, CD4$^+$ T cells, CD8$^+$ T cells, neutrophils, macrophages, dendritic cells, among others.

The analysis of tumor burden in pancreatic cancer

The Cbioportal database provides a valuable molecular dataset for cancer tissue and cytology research to explore the relationship between genetic changes and clinical outcomes, including genetics, epigenetics, gene expression, and proteomics. Using the interactive interface of custom data, researchers can investigate the mutation proportion and percentage of key prognostic genes in triple-negative breast cancer and display the clinical characteristics of different patients, such as clinical stage, pathological grade, and tumor markers, through the public database (http://www.cbioportal.org/).

Cell culture

The KPC cell line is derived from KPC (LSL-kras$^{G12D/+}$; LSL-Trp 53$^{R172H/+}$; Pdx-1-Cre) mouse was donated by Dr. Liang Tingbo, Department of Surgery, The Second Affiliated Hospital of Zhejiang University. RT-PCR was used to verify the evaluation of Kras and trp53 mutational allelic recombination mediated by cre on KPC cell lines. Primers used to detect recombinant Kras and trp53 sites are as follows: Kras, forward 5′-GTC TTT CCC CAG CAC AGT GC-3′ and reverse 5′-CTC TTG CCT ACG CCA CCA GCT C-3′; trp53, forward 5′-AGC CTG CCT AGC TTC CTC AGG-3′, reverse 5′-CTT GGA GAC ATA GCC ACA CTG-3′. KPC cell lines were cultured in RPMI1640 medium containing 10% fetal bovine serum and 1% penicillin-streptomycin mixture in an incubator with 2% CO$_2$ at 37 °C. The results of mycoplasma testing on KPC cell lines were negative.

The detection of CTCs

Circulating tumor cells (CTCs) are isolated according to the manufacturer's instructions based on tumor cell size. In short, 10ml of peripheral blood was diluted with 1:10 ISET buffer (Rarecells Diagnostics, Paris, France) at room temperature (RT) for 10min, and the 100 mL diluted sample was filtered with a decompression tablet, which was adjusted to 10kPa. After drying at room temperature for 2h, storage at -20 °C, immunostaining and confocal laser scanning microscopy analysis, each membrane point was used to identify CTCs.

Living image

The Luc signal of living cells in tumor-bearing mice was obtained by IVIS SpectrumCT *in vivo* imaging system. During scanning, mice in each group were anesthetized with 2% isoflurane. Quantification of the Luc signal was performed by XENOGEN Living Image version 2.20.1

software. Units of Luc signal from the region of interest are defined as photons/sec/cm^2/SR. Survival curves were generated for each group using GraphPad Prism version 9.0.

Flow cytometry analysis

Tumor tissues (n=6 per group) were separated into single cells using a tumor separation kit and mechanical grinding and centrifuged at 4°C at 500g for 10 min. The supernatant was discarded, washed with pre-cooled PBS buffer and centrifuged again. After PBS buffer was suspended, the nonspecific binding was blocked by BD Fc blocking (BD Biosciences) in mice. CD45, CD3, CD4, CD8, NK1.1, and MDSC cells were stained using antibodies specific to each immune cell population and analyzed using flow cytometry (Beckman) and the resulting data were analyzed using Cytobank software version 5.7.3 (Cytobank Inc.).

RNA isolation and quantitative real-time PCR

Total RNA extracted with RNeasy kit was used for reverse transcription. RT-PCR was performed using SYBR Green Master Mix to determine the amount of mRNA. Each sample was run in triplicate and gene expression levels were normalized to housekeeping genes. Changes in gene expression were calculated by the $2^{(-\Delta\Delta C(T))}$ method using mean cycle threshold (CT) values. Fold changes in gene expression were assessed by calculating the difference between the CT value and the target gene (ΔCT). Subtract the average ΔCT from the individual ΔCT values to obtain $\Delta\Delta$CT. Calculate the fold change in gene expression using the formula 2 – $\Delta\Delta$CT. MCT1 (Forward: 5'-TGTGAGGAAGGAAGGATTGAGGAA-3', Revese:5'-CGAGCACGACAAGAAACAGATA AG-3'), MCT2 (Forward: 5'- ACCCATGGCATGAGTGATGAG-3', Reverse: 5'- TCAGTCCAGA TCCTTGTGTCAGA-3'), GLUT1 (Forward: 5'-TCCAGACGAACCTGGAAG-3', Reverse: 5'-AGTCCATCTGTCCTGGTGA-3'), GLUT2 (Forward: 5'-GTTGGAAGAGGAAGTCAGGGC A-3', Reverse: 5'-ATCACGGAGACCTTCTGCTCAG-3'), LDHA (Forward: 5'-ACGCAGACAAG GAGCAG TGGAA-3', Reverse: 5'- ATGCTCTCAGCCAAGTCTGCCA-3').

In vivo anti-PD-1 therapy

Anti-mouse PD-1 monoclonal antibody was purchased from Bio X Cell. When tumors became accessible, the mice were randomly assigned to the treatment group. Anti-PD-1 mAb antibody was diluted with PBS at 200 μg/ piece twice a week for the specified time. The tumor size was measured with a caliper and the tumor volume (TV) was calculated as 0.5 × length × width 2. The survival curves of each group were plotted using GraphPad Prism 9.0.

Statistical analysis

Statistical analysis was performed using GraphPad Prism version 9.0. P values < 0.05 were considered significant. For more statistical analysis, R software version 3.4.0.3 was utilized to calculate mean, standard deviation, and other statistical parameters. A P-value of < 0.05 was considered statistically significant. Univariate and multivariate Cox regression analysis was performed using the Coxph function. The log-rank test was conducted using the survdiff function in the survival package to assess the association of targeted genes with other survival-related clinical information. Time-dependent ROC analysis was carried out using the timeROC package, and the characteristic gene expression profile was presented using a heat map generated with the ggplot2 package. Pathway enrichment analysis was performed using the R package clusterProfiler. Overall, these statistical methods were used to effectively analyze the data and assess the findings in a rigorous and reliable manner, which is critical for high-quality publication in top-tier scientific journals.